

Self-Propulsion of N-Hinged 'Animats' at Low Reynolds Number

Gerusa Alexsandra de Araújo*

*Laboratório Nacional de Computação Científica,
Av. Getúlio Vargas 333, Petrópolis, RJ,
25651-070 Brazil.
E-mail: gerusa@lncc.br*

and

Jair Koiller†

*Fundação Getúlio Vargas,
Praia de Botafogo 190, Rio de Janeiro, RJ,
22253-900, Brazil.
E-mail: jkoiller@fgv.br*

Submitted: June 30, 2003 Accepted: November 25, 2003

Dedicated to Jorge Sotomayor on his 60th birthday

Optimal locomotion of micro-organisms (on a small Reynolds number flow) can be regarded as a sub-riemannian geometry on a principal bundle with a mechanical connection. Aiming at robotic applications, flagella are modeled as concatenated line segments with variable hinge angles. As an example, we consider E. Purcell's 2-hinged animat [39], the simplest configuration capable to circumvent Stokes flow reversibility.

Key Words: Stokes flows, connections and curvature, nonholonomic constraints.

MCS2001: 76D07,76Z10,93B29,93C10,51P05,53C05

PACS-1990: 47.15Gf,87.45.-k,87.10.+e,02.40.+m,03.40.Gc

* On a CNPq/Brazil Ph.D. fellowship at LNCC.

† Partially supported by a CNPq research fellowship 30007-83/3.

1. INTRODUCTION.

1.1. A “gauge-theory” for microswimming.

About 2.5×10^2 years ago d’Alembert and Lagrange considered mechanical problems with linear constraints in generalized velocities. Lagrange-d’Alembert’s principle states that constraint reaction forces produce no work. The generic case of nonintegrable constraints is called “nonholonomic mechanics”.

On the other hand, if a variational principle (subject to the constraints) is used, one gets “vakonomic mechanics”, in the nice terminology (variational axiomatic) coined Arnold’s school [1]. Hertz [17] already knew that, although using the same ingredients, the two mathematical theories, nonholonomic and vakonomic, are quite different: in nonholonomic mechanics, trajectories follow the *straightest* paths satisfying the constraints, whereas in vakonomic mechanics they follow the *shortest paths*. But unless the constraints are holonomic, straightest are not the same as shortest paths!

In Mechanical Engineering most applications are of nonholonomic (that means, of Lagrange-d’Alembert) type; in contradistinction, most applications in Control Engineering require vakonomic mechanics. Although one would think that the former is the oldest, actually it is rather the opposite. Applications of vakonomic mechanics started about 4.0×10^9 years ago!

In fact, as outlined in the programme described in [20], *optimal microswimming is a sub-riemannian geometry*¹. Flagellar locomotion was left aside in the previous studies of our group [20, 21, 22, 23, 12, 13, 24], and so will be the object of this paper.

The main object is a *connection 1-form*. The main point of this paper is to show that the computation of the “Stokes connection” is feasible. For simplicity, we will use the resistive theory for flagellary motion, [50]. The geometric approach can be combined with more refined fluid mechanics, but in practice the resistive-force approximation is adequate [9].

1.2. Historical remarks.

Following ideas presented by E. Purcell at the 1976 annual APS meeting [39], Shapere and Wilczek proposed in 1989 a “gauge-theory” for swimming at low Reynolds numbers [43, 44, 45]. Using analytical techniques for Stokes flows they revisited ciliary locomotion of a spherical cell under the “envelope” approximation [25, 3]. Building up along their lines, we proposed a sub-riemannian geometry research programme for microswimming, which we pursued in the above mentioned papers, and we considered more general basic shapes.

¹See [31] for background in Geometric Mechanics and [32] for Sub-riemannian Geometry. For a dictionary between optimal control, gauge theory and sub-riemannian geometry, see [33].

Although a convenient geometric language did not exist in the early 50's, the underlying structure was already clear to G.I. Taylor [48] and J. Lighthill [25], the founding fathers of "mathematical biofluidynamics". For the period 1950-1975 we refer to the wonderful book [26] and the reviews by Lighthill [27, 28]. Until the the mid 70's the fluid mechanics community produced a steady flow of publications on flagellated hydrodynamics; as a sample of the literature see e.g., [4, 5, 6, 7, 8, 19, 18], and the proceedings of the special year at Caltech in 1974 organized by Prof. T.Wu, C. Brennen, and C. Brokaw [50]. Somehow the effort diminished later on; according to Prof T.Wu (personnal communication), most questions posed at that time by biologists were answered.

However, in the last ten years, new techniques in cell biology, specially those related to optical tweezers, are producing exciting results and a new agenda. For a glimpse of the recent literature, see [34, 49, 46, 47, 41, 42, 37, 10]. Certainly, these developments will stimulate a renewed surge of interest in the mathematical study of cellular motion.

1.3. A earlier optimization attempt.

In the proceedings of the 1974 Caltech interdisciplinary year on "Swimming and Flying in Nature", [35], and in a subsequent paper published in the Journal of Fluid Mechanics, [36], Pironneau and Katz posed the problem of minimizing the power expenditure in flagellar locomotion as follows:

"Given that a (flagellated) organism swims from A to B in a given time, what is the most economical way of doing so? Our notion of economy is thus a purely hydrodynamical one, although our results are potentially useful in the study of flagellar contraction mechanisms themselves" ... The methods of optimal control theory are used in seeking those motions which propel an organism at a prescribed speed while minimizing its instantaneous rate of hydrodynamical working" [35].

Hence they regarded the problem as

"an optimal control problem of a non-standard type, for which no general theory has been developed ... the problem is non-standard in the sense of optimal control theory in that the boundaries are not stationary [36]".

Fâute de mieux, they decided to study a simplified problem:

"We shall therefore solve an alternative, though closely related problem in which the instantaneous rate of working is minimized at each time" [35].

We assert that any such *instantaneous* optimality criterion is doomed. Since Stokes flows are reversible, for a net motion to occur, a full non-reversible cycle in "shape space" must be taken into account². Any rea-

²One observes frequently in video microscopy that many organisms seem to go backwards in part of the cycle; perhaps this common feature is present even in optimal motions.

sonable definition of *efficiency*, e.g., those considered by Lighthill [25] and Shapere/Wiczek [45], use the *full swimming cycle*. A technical issue, but also important, is the assumption of a constant forward velocity in [35, 36]. To be fair, there is one situation in which the assumptions of PK work: an organism powered by a rotating rigid flagellum; but this can be studied directly as in [40].

Summarizing: there is a serious difficulty in reconciling instantaneous with *overall* motion optimization. This is due to the inherent reversibility of Stokes flows. In our viewpoint, *geometrical control theory* is the natural tool for studying microorganism locomotion.

1.4. Purcell's paper

E. Purcell coined a delicious terminology (delicious in all senses of the word): the “scallop paradox”. It describes a no-go situation that results from any reciprocal strategy.

Navier - Stokes :

$$-\nabla p + \eta \nabla^2 \vec{v} = \cancel{\rho \frac{\partial \vec{v}}{\partial t}} + \cancel{\rho (\vec{v} \cdot \nabla) \vec{v}}$$

If $Re \ll 1$:

Time doesn't matter. The pattern of motion is the same, whether slow or fast, whether forward or backward in time.

The Scallop Theorem



FIG. 1. Adapted from Fig.5 of [39]. See quotation.

“Life at low Reynolds number” [39], is one of the 1977 American Journal of Physics memorable papers (continued posthumously in [40]). The reader is challenged to describe the motion of the *animat* depicted in Fig. 2. Together with Fig. 1, also from that paper, the key features of zero Reynolds number locomotion are masterfully explained.

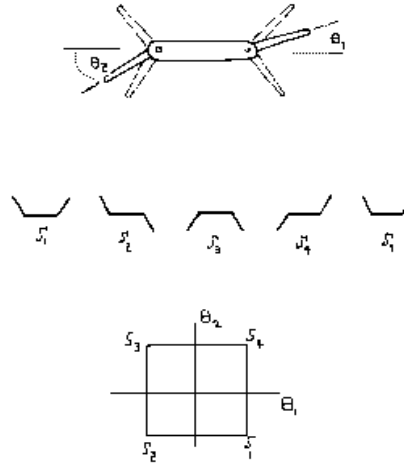


FIG. 2. Adapted from Fig.7 of [39]. See quotation.

“There is a very funny thing about motion at low Reynolds number, which is the following. One special kind of swimming motion is what I call a reciprocal motion. That is to say, I change my body into a certain shape and then I go back to the original shape by going through the sequence in reverse. At low Reynolds number, everything reverses just fine. Time, in fact, makes no difference—only configuration. If I change quickly or slowly, the pattern of motion is exactly the same. If you take the Navier-Stokes equation and throw away the inertia terms, all you have left is $\Delta v = \nabla p / \eta$, where p is the pressure (η is the viscosity). So, if the animal tries to swim by a reciprocal motion, it can't go anywhere. Fast or slow, it exactly retraces its trajectory and it's back where it started. A good example of that is a scallop. You know, a scallop opens its shell slowly and closes its shell fast, squirting out water. The moral of this is that the scallop at low Reynolds number is no good.

It can't swim because it only has one hinge, and if you have only one degree of freedom in configuration space, you are bound to make a reciprocal motion. There is nothing else you can do. The simplest animal that can swim that way is an animal two hinges. I don't know whether one exists but Fig. 7 shows a hypothetical one. This animal is like a boat with a rudder at both front and back, and nothing else. This animal can swim. All it has to do is go through the sequence to configurations shown, returning to the original one at S_5 . Its configuration space, of course, is two dimensional with coordinates θ_1, θ_2 . The animal is going around a loop in that configuration space, and that enables it

to swim. In fact, I worked this one out just for fun and you can prove from symmetry that it goes along the direction shown in the figure. As an exercise for the student, what is it that distinguishes that direction?"

We present here an algorithm to perform simulations for this problem, see section 3. This algorithm is based on simple linear algebra rules governing the velocities/angular velocities and forces/torques in “Aristotelian physics” (section 2). The main goal of this paper is to produce a Hamiltonian system giving the *optimal* motions of a flagellated organism or robot with N hinges ($N + 1$ links), see Fig. 3. This is done in section 4.

We will present elsewhere a detailed report on the numerical experiments, but we present two some illustrative simulations in section 6, showing that even the simplest case, Purcell’s animat, already presents quite unexpected motions³. Purcell’s intuition about the overall motion is indeed remarkable!

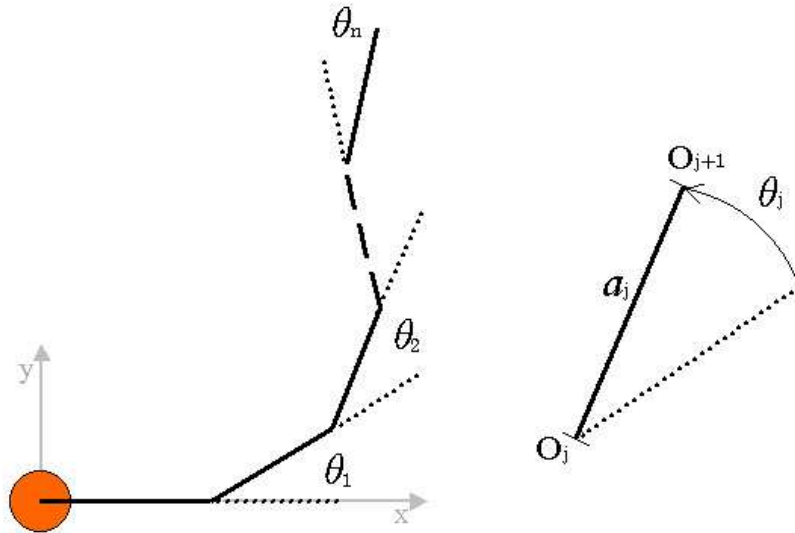


FIG. 3. Configuration space for the planar N -hinged swimmer. Shape variables are $\theta_1, \dots, \theta_N$. $SE(2)$ variables are x, y, ϕ , where (x, y) are the coordinates of the cell center and ϕ the angle of rod a_0 with the x -axis. A motion plan $\{\theta_j(t)\}$ is lifted to a curve of located shapes satisfying the constraints of zero total force and torque.

The reader may amuse himself (herself) with the simple .m file presented in the appendix to simulate the 2-hinged Purcell swimmer. We have similar .m files for the case of $N \geq 3$ hinges. A graphic interface is currently being

³As this paper was being written, Greg Huber called our attention to the preprint by H.Stone et al. [2], which describe similar results on Purcell’s animat.

prepared to generate and depict movies of the motions. The next stage is searching for efficient motion plans via genetic algorithms. A more ambitious project (quite intensive computationally), which we plan to pursue futuere, is a numerical study of the Hamiltonian system giving the optimal motions.

2. ARISTOTELIAN PHYSICS.

The rise of modern mechanics was an event of monumental magnitude, leaded by Galileo and Newton. over the last 300 years, students learn that forces (torques) are proportional to linear (angular) accelerations, instead of linear (angular) velocities. Nonetheless, the Aristotelian viewpoint, seems somehow to be the default software in college students brains. “We have to first unteach them their world view of physics, which dates all the way back to Aristotle” [11].

We think that this frame of mind represents “fossil memories” so it could actually be fair to pursue a little bit of Aristotelian physics in classroom. After all, it dominated for more than 3 billion years: as far as life at zero Reynolds is concerned, Aristoteles *is* right⁴. Moreover, there are many important phenomena in the zero Reynolds regime, from cellular biology to chemical/environmental engineering (sedimentation processes of particles in fluids).

Our configuration space \mathcal{Q} consists of all rigid bodies $q = \mathcal{B}$ inside the 3-dimensional *affine* space. We may fix an origin O and a reference frame $Oxyz$. We identify an element $q = \mathcal{B}$ by the position $\mathbf{r}_{OP} \in \mathbf{R}^3$ of a distinguished material point P on the body together with the attitude matrix $R \in SO(3)$ of a frame attached in the body:

$$\mathcal{B} \leftrightarrow (\mathbf{r}_{OP}, R) . \quad (1)$$

Shapes of bodies will be important in the sequel, but no further information is needed momentarily. Thus the space of all located shapes will be denoted \mathcal{Q} . If we first apply a rotation $S \in SO(3)$ *about* P to the body, and after that we apply a translation $b \in \mathbf{R}^3$, it will reach the configuration

$$g \cdot \mathcal{B} \leftrightarrow (\mathbf{r}_{OP} + b, SR) . \quad (2)$$

Now, if we apply an infinitesimal rotation ω about P and an infinitesimal translation \mathbf{t} , any point Q in the body will have a linear velocity given by $\omega \times \mathbf{r}_{PQ} + \mathbf{t}$. Mathematically, this operation represents the action on $Q \in \mathcal{B}$ by the element (ω, \mathbf{t}) of the Lie algebra $se(3)$. The affine structure

⁴If a bacterium flagellum stops rotating, it will coast about 0.1 angstrom in 0.6 microseconds [39].

is manifested on the arbitrariness of choice of origin P . We will present below (Proposition 2) the rules of transformation when another origin is taken.

If the body moves on fluid and the Reynolds number is so small that the inertial effects can be neglected, we are in the realm of Aristotelian physics: whenever the body is subjected to an external force \mathbf{F} and torque \mathbf{T}_P about the point P , there is a *linear relationship* between $(\mathbf{F}, \mathbf{T}_P)$ and (\mathbf{U}_P, ω) . Properties of this map were elucidated by Happel and Brenner[16].

Fix an origin O .

DEFINITION 1. The *resistance operator* (Purcell calls them “propulsion” operator) is given by a 6×6 positive definite matrix $\mathbf{G} = \mathbf{G}_O$ (3×3 in the 2-dimensional case)

$$\mathbf{G}_O = \mathbf{G}(\mathcal{B}, O) = \mu \begin{pmatrix} \mathbf{K} & \mathbf{C}_O^\dagger \\ \mathbf{C}_O & \mathbf{\Omega}_O \end{pmatrix} \quad (3)$$

such that

$$\begin{pmatrix} \mathbf{F} \\ \mathbf{T}_O \end{pmatrix} = \mathbf{G} \cdot \begin{pmatrix} \mathbf{U}_O \\ \omega \end{pmatrix} \quad (4)$$

where μ is the viscosity. The latter indicates the instantaneous translational velocity $\mathbf{t} = \mathbf{U}_O$ of the body and its rotational angular velocity ω about that point O .

It is very important to take note of transformation rules related to the change of origin. Choose another point P through which both axis of rotation ω and torque \mathbf{T}_P are taken (P can be the distinguished point if we wish). There is a similar equation to (4) where the subscript P replaces O :

$$\begin{pmatrix} \mathbf{F} \\ \mathbf{T}_P \end{pmatrix} = \mu \begin{pmatrix} \mathbf{K} & \mathbf{C}_P^\dagger \\ \mathbf{C}_P & \mathbf{\Omega}_P \end{pmatrix} \cdot \begin{pmatrix} \mathbf{U}_P \\ \omega \end{pmatrix} \quad (5)$$

An elementary (but fundamental) fact is a *duality* between motions (geometry) and forces (physics).

- \mathbf{U}_O depends on the choice of origin:

$$\mathbf{U}_P = \mathbf{U}_O + \omega \times \mathbf{r}_{OP} \quad (6)$$

ω is a “free vector” (it may set to pass either through point O or P).

- \mathbf{T}_O depends on the choice of origin:

$$\mathbf{T}_P = \mathbf{T}_O + \mathbf{F} \times \mathbf{r}_{OP} \quad (7)$$

\mathbf{F} does not depend on the choice of origin (“free”).

The duality between (\mathbf{U}_O, ω) and $(\mathbf{F}, \mathbf{T}_O)$ means that the inner product

$$\mathbf{Power} = \mathbf{F} \cdot \mathbf{U}_O + \mathbf{T}_O \cdot \omega = \mathbf{F} \cdot \mathbf{U}_P + \mathbf{T}_P \cdot \omega \quad (8)$$

does not depend on the choice of origin. This quantity represents the *hydrodynamical power expenditure* and is the integrand of the optimality functional.

The power expenditure equation expresses mathematically that velocities (linear and angular) are tangent vectors, while forces/torques are co-tangent objects. Consequently, they have dual laws of transformation.

The proof is easy. Note that the net velocity \mathbf{u} at every point Q (in the affine space) must satisfy

$$\mathbf{u} = \mathbf{U}_O + \omega \times (Q - O) = \mathbf{U}_P + \omega \times (Q - P)$$

from which (6) follows. The relationship between torques about two different points is a well know result from elementary physics (Steiner’s theorem) and follows by inserting (6) into the duality equation (8). The power expenditure is *quadratic* in the velocity, and we define the inner product of $\mathbf{v}_1 = (\mathbf{U}_1, \omega_1)_P$ and $\mathbf{v}_2 = (\mathbf{U}_2, \omega_2)_P$ by

$$\langle \mathbf{v}_1, \mathbf{v}_2 \rangle = (\mathbf{U}_1, \omega_1)_P \mathbf{G}_P \begin{pmatrix} \mathbf{U}_2 \\ \omega_2 \end{pmatrix}_P \quad (9)$$

Rules for matrix transformation under changes of *coordinate frames* and origin can be easily derived. For planar motions, these rules are encoded by 3×3 matrices $M(x, y, \phi)$.

PROPOSITION 2. Consider an infinitesimal planar motion $(\omega, \mathbf{V})_{Oxy} \in sE(2)$, referred to origin and frame Oxy . This same infinitesimal motion, referred to a different origin $P = (x, y)$ (given in terms of Oxy coordinates) and frame rotated by an angle ϕ , is described by $(\mathbf{v}, \omega)_{(P, \phi)}$, where

$$\begin{pmatrix} \mathbf{v} \\ \omega \end{pmatrix}_{(P, \phi)} = M \begin{pmatrix} \mathbf{V} \\ \omega \end{pmatrix}_{(0, \phi=0)} \quad (10)$$

where

$$M(x, y, \phi) = R(-\phi)T(x, y) \quad (11)$$

and

$$R(\phi) = \begin{pmatrix} \cos \phi & -\sin \phi & 0 \\ \sin \phi & \cos \phi & 0 \\ 0 & 0 & 1 \end{pmatrix}, \quad T(x, y) = \begin{pmatrix} 1 & 0 & -y \\ 0 & 1 & x \\ 0 & 0 & 1 \end{pmatrix} \quad (12)$$

Dually, the transformation laws for forces and torques are given by the transpose M^\dagger

$$\begin{pmatrix} \mathbf{F} \\ \tau \end{pmatrix}_{(O, \phi=0)} = T(x, y)^\dagger R(\phi) \begin{pmatrix} \mathbf{F} \\ \tau \end{pmatrix}_{((x, y), \phi)} \quad (13)$$

From these basic results we can easily derive the transformation rules for resistance matrices, when the base point is changed. For our purposes we will use only the examples below, of basic importance for our computational scheme.

EXAMPLE 3. Stokes laws: the translational resistance coefficient of a spherical cell of radius r is $6\pi\mu r$ and the rotational coefficient is $8\pi\mu r^3$. Resistance coefficients for spheroidal cells can be found in [16].

EXAMPLE 4. The general solution for Stokes flows past a general tri-axial ellipsoid has been found analytically, and by taking limits, approximate formulas for slender rods have been derived. For an elongated body with total length $2a$ and maximum local radius b , $F_T = C_T 2a$, $F_N = C_N 2a$ where

$$C_T \sim \frac{2\pi\mu}{\ln(a/b) - 0.5}, \quad C_N \sim \frac{4\pi\mu}{\ln(a/b) + 0.5} \quad (14)$$

(see [16], (5-11.50) and (5-11.54)). It follows that the resistance matrix, giving the force and torque components referred to the center point (at the origin) of a rod of length a placed horizontally, is given by the diagonal matrix

$$D = \begin{pmatrix} C_T a & 0 & 0 \\ 0 & C_N a & 0 \\ 0 & 0 & C_N a^3/12 \end{pmatrix}$$

That the torque coefficient must be $\kappa = C_N a^3/3$ follows simply by a *consistency* argument:

$$a^3 \kappa \omega = 2 \int_0^{a/2} x(\omega x) C_N dx = 2 C_N \omega a^3/24 \implies \kappa = \frac{1}{12} C_N.$$

This same resistance operator, referred to the *left endpoint*, is given by $G_o(a; C_T, C_N) = M^T D M$, where

$$M = \begin{pmatrix} 1 & 0 & 0 \\ 0 & 1 & a/2 \\ 0 & 0 & 1 \end{pmatrix}.$$

It follows that

$$G_o = \begin{pmatrix} C_T a & 0 & 0 \\ 0 & C_N a & C_N a^2/2 \\ 0 & C_N a^2/2 & C_N a^3/3 \end{pmatrix}. \tag{15}$$

EXAMPLE 5. As we saw above, the resistance coefficients for a smooth flagellum in the resistive approximation obey the approximate relationship [27]

$$C_T/C_N \sim \frac{1}{2}, \tag{16}$$

but this relationship can change drastically. Fig. 4 depicts a flagellum with *mastigonemes*. Consider a rectilinear segment of flagellum of length a and suppose there are K mastigonemes per unit length, each of length b .

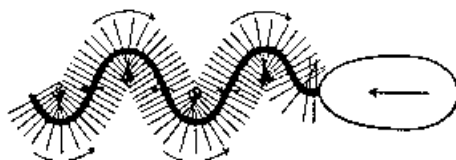


FIG. 4. The cumulative effect of the presence of mastigonemes along the flagellar axis makes the net axial resistance coefficient greater than the transversal coefficient. Waves propagating from base to tip produce locomotion in that direction. In a smooth flagellum, such waves produce motions in the opposite direction.

It is easy to verify that the longitudinal force is given by

$$F_T = (C_T a + C_N b(Ka)) v_T \tag{17}$$

and that the transversal force is

$$F_N = (C_N a + C_T b(Ka)) v_N \tag{18}$$

Therefore

$$\begin{pmatrix} C_T^m \\ C_N^m \end{pmatrix} = \begin{pmatrix} 1 & bK \\ bK & 1 \end{pmatrix} \begin{pmatrix} C_T \\ C_N \end{pmatrix} \tag{19}$$

so

$$C_T^m/C_N^m = \frac{C_T/C_N + bK}{bK C_T/C_N + 1} \tag{20}$$

and therefore

$$K \rightarrow \infty \text{ implies } C_T^m / C_N^m \rightarrow C_N / C_T . \quad (21)$$

Summary: the point of this section is that there is a duality between the transformations rules for linear velocities (and angular velocities) and the rules of transformations for forces (and torques). This is true also in Newtonian physics, but in Aristotelian physics, there is, additionally, a linear map - the resistance operator - from the (velocity, angular velocity) space to its dual (force, torque)-space.

3. RECONSTRUCTION OF LOCATED SHAPES: CONNECTION FORM

The fundamental insight for self propulsion at low Reynolds number was masterfully summarized by J. Lighthill in his 1975 John von Neumann lecture [27]:

“The organism’s motile activity, in fact, is able to specify the instantaneous rate of deformation of its external surface only *to within an arbitrary rigid-body movement*. That movement, comprising a translation and a rotation, is uniquely determined by the requirement that the forces between the body and the fluid form a system of forces with zero [force] resultant and zero moment”.

For definiteness, we will restrict the discussion to flagellar locomotion in a two dimensional plane inside \mathcal{E} . Everything extends, in a straightforward but more numerically intensive (the matrices will be 6×6) manner, to three dimensional motions. We begin by setting up our terminology.

DEFINITION 6. *Input functions:* A *motion plan* is defined by a set of N periodic *functions* $\theta(t) = (\theta_1(t), \dots, \theta_N(t))$, $0 \leq t \leq T$. The closed curve $\theta(t)$ determines a trajectory in the space of *unlocated shapes* \mathcal{S} . We define the *standard gauge* as the located shape in which the center of the cell is always at the origin (say, forced by a lazer tweezer) and the attitude angle is $\phi \equiv 0$. The space of all located shapes is the product $\mathcal{Q} = SE(2) \times \mathcal{S}$.

In differential geometric language, \mathcal{Q} is the total space of a principal $SE(2)$ -bundle over the base space \mathcal{S} .

DEFINITION 7. *Input parameters:*

- The lengths of the $N + 1 \geq 2$ straight segments a_i ($i = 0, \dots, N$)
- The cell radius r .
- The resistance coefficients C_T and C_N .

DEFINITION 8. *Output functions;* There are three *output* or *reconstruction* functions $(x(t), y(t), \phi(t)) \in SE(2)$. The first two give the coordinates

of the center of the cell, and the *attitude* $\phi(t)$ is the angle of the first segment with the x-axis. The output functions, together with the input functions, specify the located shape at any given time.

Our algorithm requires, as intermediary steps, the calculation of the following functions of $\theta_j(t)$.

DEFINITION 9. *Intermediary functions:*

- The *resistance matrix* G (3×3), an operator that gives the force and torque corresponding to a rigid motion of the flagellum “frozen” at the current shape, as discussed in the previous section.
- The *forcing matrix* A ($3 \times N$), an operator that gives the force and torque due to the shape change $\dot{\theta}_j$ ($j = 1, \dots, N$) at the standard gauge.
- The *metric matrix* K ($N \times N$), which gives the hydrodynamical power expenditure (of admissible motions)

With G and A on hand we are able to write down the *reconstruction algorithm*: for any motion plan, there is a corresponding curve of located shapes (the “horizontal lift”)

$$\theta_j(t) \ 1 \leq j \leq N \implies (x(t), y(t), \phi(t)) \in SE(2) .$$

For its reconstruction, we need only the *connection matrix*

$$C = -G^{-1}A \ (3 \times N). \quad (22)$$

With C and K on hand, we can write a *Hamiltonian system* giving the optimal motion plans. It yields (as one should expect and we show in the next section) a second order ODE for the $\theta_j(t)$. An important feature is the existence of three constants of motion p_x, p_y, p_ϕ which allow trajectories to reach all points of the $N+3$ dimensional configuration space $(\theta_1, \dots, \theta_n, x, y, \phi)$.

In mathematical terms, the implication from Lighthill’s statement quoted above is that in 2-dimensions, these are linear constraints for the admissible infinitesimal displacements of elements of \mathcal{Q} . In modern language, they define a *connection* on the the space of located shapes⁵.

The infinitesimal translation and rotation of the cell body resulting from an infinitesimal shape change $\dot{\theta}_j$, $1 \leq j \leq n$ is given by

$$(v_1, v_2, \dot{\phi})^\dagger = C \dot{\theta} \quad (23)$$

⁵We are thinking of two dimensional motions inside \mathbf{R}^3 , so here there is none of the technical difficulties associated to the Stokes paradox as discussed in [44] and [20].

It is very important to notice that at any particular time instant, the body is already at a rotated position,

$$R(\phi) = \begin{pmatrix} \cos(\phi) & -\sin(\phi) \\ \sin(\phi) & \cos(\phi) \end{pmatrix} .$$

Thus, if we denote by $e_1(\phi)$ and $e_2(\phi)$ the column vectors of $R(\phi)$, then the infinitesimal translation is given by the vectorfield

$$(\dot{x}, \dot{y}) = v_1 e_1 + v_2 e_2 , \tag{24}$$

where

$$v_1 = C_{11} \dot{\theta}_1 + \dots + C_{1N} \dot{\theta}_N , \quad v_2 = C_{21} \dot{\theta}_1 + \dots + C_{2N} \dot{\theta}_N \tag{25}$$

The equation for the attitude $\phi(t)$ decouples:

$$\phi(t) = \phi_o + \int_0^t C_{31} d\theta_1 + \dots + C_{3N} d\theta_N \tag{26}$$

By Stoke's theorem, the latter can be also written as a double integral in $d\theta_i \wedge d\theta_j$.

Thus it is possible to solve equation (24) by quadrature, yielding the cell center position $(x(t), y(t))$.

Remark 10. Gauge theory experts would say that this is an exceptional case in which a path ordered integral can be exactly computed. In three dimensions a quadrature is not feasible in general, so one must solve numerically a time dependent system of linear ODEs, which has the form of $\dot{g} = gX(t)$, with $g \in SE(3)$ for a given curve $X(t)$ in the Lie algebra.

Why $C = G^{-1}A$? We now state our basic result:

PROPOSITION 11. *The connection formula. In self propulsion, in terms of our standard gauge, at any time instant one has*

$$\underbrace{G \begin{pmatrix} v_1 \\ v_2 \\ \dot{\phi} \end{pmatrix}}_{\text{force due to rigid motion}} + \underbrace{A \begin{pmatrix} \dot{\theta}_1 \\ \dots \\ \dot{\theta}_N \end{pmatrix}}_{\text{force due to shape deformation}} = 0 \tag{27}$$

hence $C = -G^{-1}A$ (note the minus sign!).

4. OPTIMAL MOTIONS.

Recall that a *sub-Riemannian geometry* consists of a *metric* (i.e, a Lagrangian L on a configuration space \mathcal{Q} consisting only on the kinetic energy term T), together with a *constraints* distribution, i.e, a linear subspace of every tangent space. A special case of interest is when a symmetry group G acts on \mathcal{Q} and the constraints define a connection on a bundle $\mathcal{Q} \rightarrow \mathcal{S}$. In differential geometric jargon, we have a vector bundle of *horizontal spaces* consisting of the admissible infinitesimal motions. In our case, the Lagrangian is given by the hydrodynamical dissipation (which is, indeed, quadratic in the velocity) and the admissible infinitesimal changes of located shapes (those for which the total force and total torque vanish).

We use the standard notation for tangent vectors from differential geometry and nonlinear control theory: vectors act on functions by directional derivative, $\partial/\partial x_j$ denotes the vector such that $\partial/\partial x_j \cdot f = \partial f/\partial x_j$ in coordinates (x_1, \dots, x_n) .

Motions in which the body do not change shape are called rigid or *vertical* motions in \mathcal{Q} . The vertical fibers are diffeomorphic to the euclidian group. The base space of this bundle is called the *shape space*.

There are two geometrical facts that are fundamental here, see [20].

PROPOSITION 12. *The connection form is of “mechanical type” and has full curvature. More precisely,*

1. *The infinitesimal vertical motions are perpendicular (with respect to the power expenditure metric) to the admissible motions. We say that the connection is of “mechanical type”.*

2. *The horizontal spaces are fully nonintegrable (also said to be fully non-holonomic.)*

Remark 13. i) By Chow’s theorem of nonlinear control theory [32], it follows that every pair of located shapes can be connected by a piecewise smooth admissible path. ii) That connections on a constrained problem are frequently of mechanical type with regards to underlying metric is a most remarkable feature [31]. In our problem, this follows from the *reciprocity* formula for Stokes equations, found by H.A. Lorentz in 1907, which is analogous to Green’s identity in potential theory. A proof of the second statement is in order; (for us this fact is a question of faith). Indeed, an interesting research project would be to compute the Lie bracket filtration in the general case. For Purcell’s animat, we believe it will realize of Cartan’s famous 2-3-5 distribution.

We can now give the recipe for the Hamiltonian. First, we take a basis of vectorfields X_1, \dots, X_N for the horizontal spaces, given by

$$X_j = \partial/\partial \theta_j + c_{1j}e_1(\phi) + c_{2j}e_2(\phi) + c_{3j}\partial/\partial \phi, \quad 1 \leq j \leq N. \quad (28)$$

That X_j are horizontal follows immediately from (23).

Any located shape infinitesimal change can be written

$$v = u_1 X_1 + \dots + u_N X_N + z_1 e_1 + z_2 e_2 + z_3 \partial/\partial\phi . \quad (29)$$

As we saw, it follows from the Lorentz reciprocity formula that the horizontal vectors X_j are perpendicular to the vertical displacements

$$\partial/\partial x, \partial/\partial y, \partial/\partial\phi .$$

It is important to take note of the coordinate change formulae. Vector v can also be written

$$v = v_q = \dot{\theta}_1 \partial/\partial\theta_1 + \dots + \dot{\theta}_N \partial/\partial\theta_N + w_1 e_1 + w_2 e_2 + w_3 \partial/\partial\phi, \quad (30)$$

where $w_3 = \dot{\phi}$ (and $w_1 = \dot{x}$ when $e_1 = \partial/\partial x$, $w_2 = \dot{y}$ when $e_2 = \partial/\partial y$). It is immediate to see that $u_j = \dot{\theta}_j$ and

$$\begin{aligned} z_1 &= w_1 - (c_{11}\dot{\theta}_1 + \dots + c_{1N}\dot{\theta}_N) \\ z_2 &= w_2 - (c_{21}\dot{\theta}_1 + \dots + c_{2N}\dot{\theta}_N) \\ z_3 &= \dot{\phi} - (c_{31}\dot{\theta}_1 + \dots + c_{3N}\dot{\theta}_N) . \end{aligned} \quad (31)$$

Now, we enforce the constraints by introducing a penalization on vertical motions. Let $\lambda \rightarrow \infty$ a increasingly large parameter. The *penalized Lagrangian* is given by (the factor of 2 is just for convenience)

$$L_\lambda(v, v) = \frac{1}{2} \sum_{i,j=1,\dots,N} k_{ij} u_i^2 u_j^2 + \lambda(\text{fiber metric}) \quad (32)$$

where (the brackets below indicate the power expenditure metric)

$$k_{ij} = \langle X_i, X_j \rangle \quad (33)$$

The rationale is to make motions along the fiber (i.e., rigid displacements, without any change of shape) extremely expensive. As $\lambda \rightarrow \infty$, we expect that $z_1, z_2, z_3 \rightarrow 0$ on the optimal motions, so from equations (31) the constraints are enforced.

Furthermore, since the Lagrangian L_λ is invariant under the euclidian group $SE(2)$, by Noether's theorem, we get the three usual conserved momenta:

$$p_x, p_y, p_\phi$$

whose expressions in terms of the velocities will be given shortly, see (37) below.

The Legendre transformation from the generalized velocities u_j (also called “quasi-velocities” in the nonholonomic systems literature) velocities to their corresponding momenta m_j is given by

$$(m_1, \dots, m_N)^\dagger = K \cdot (u_1, \dots, u_N)^\dagger \tag{34}$$

The m_j are the ordinary momenta p_{θ_j} with added “magnetic type” terms,

$$m_j = p_{\theta_j} + c_{1j}p_x + c_{2j}p_y + c_{3j}p_\phi, \quad 1 \leq j \leq N. \tag{35}$$

This follows from equations (29, 30, 31), by dualization.

Here is the punch line:

PROPOSITION 14. *Optimal motions:*

1. *Optimal motions obey the Hamiltonian system, depending on parameters p_x, p_y, p_ϕ , defined on the reduced phase space $\{(\theta_1, \dots, \theta_N, p_{\theta_1}, \dots, p_{\theta_N})\}$ with Hamiltonian*

$$H = \frac{1}{2}(m_1 \dots m_N) \begin{pmatrix} k_{11} & \dots & k_{1N} \\ \dots & \dots & \dots \\ k_{N1} & \dots & k_{NN} \end{pmatrix}^{-1} \begin{pmatrix} m_1 \\ \dots \\ m_N \end{pmatrix}. \tag{36}$$

2. *The conserved momenta $p_x p_y p_\phi$ are given in terms of the velocities by*

$$\begin{pmatrix} p_x \\ p_y \\ p_\phi \end{pmatrix} = \mathbf{G} \begin{pmatrix} \lambda z_1 \\ \lambda z_2 \\ \lambda z_3 \end{pmatrix} \tag{37}$$

where \mathbf{G} , in our problem, is the resistance operator.

It is important to notice that as $z_1, z_2, z_3 \rightarrow 0$ and $\lambda \rightarrow \infty$ in such a way that the conserved momenta may have finite, arbitrary, values.

Remark 15. Hertz already noticed in his book [17] on the “Foundations of Mechanics”, that constrained variational problems must, and will, have such compensating features. The space of allowed infinitesimal motions has co-dimension three (there are three constraints). The presence of three arbitrary parameters provides a three dimensional pencil of solutions for every initial position and admissible velocity. Therefore, it remains possible that every pair of points in the configuration space of located shapes to be joined by a sub-Riemannian geodesic (actually, by a zig-zag of such arcs). For technical details, see Montgomery[32].

5. THE MATRICES G , A , K

This section contains our best kept secrets. As we saw in section 3, all the relevant quantities (torques and translational velocities) will be referred to a *same* origin and frame. We found to be convenient choosing 0 (the center of the cell) and the standard gauge $\phi = 0$. Changes of origin and frame are easily implemented, multiplying by matrices of type M on the right (see (11) and Proposition 2) and M^\dagger on the left.

We make use of an approximate *additivity property* (see Purcell[39], Figs.13 and 14): “if two ... devices ... are far enough from one another so that their velocity patterns don’t interact, their propulsive matrices just add”. Actually this result is mathematically valid to first order, even if the pieces in consideration are close to each other. In the context of flagellar motion, this follows from slender body approximation formulas by Lighthill [29]. Therefore, we can write the resistance matrix as a sum of positive definite matrices

$$G = G_{cell} + G_o + G_1 + \dots + G_N, \quad (38)$$

where the G_k can be recursively computed using the positions O_k of the k -th pivot and the angle ϕ_k of the k -th segment with the x-axis:

$$\phi_o = \theta_o = 0, \quad \phi_j = \phi_{j-1} + \theta_j, \quad 1 \leq j \leq N \quad (39)$$

$$O_o = 0, \quad O_j = O_{j-1} + a_{j-1} \exp(i\phi_{j-1}), \quad 1 \leq j \leq N \quad (40)$$

$$G_o = G_o(a_o), \quad G_k = T^t(O_k)R(\phi_k)G_o(a_k)R(-\phi_k)T(O_k) \quad (41)$$

The cell resistance matrix G_{cell} (see Example 3) may or may not be included.

To compute the $3 \times N$ momentum matrix A , note that its k -th column A^k gives the two force components and by the torque (referred to O and gauge $\phi = 0$) produced by the angular rotation (with angular velocity = 1) around the k -th hinge. Using the same general recipe for (38), we compute the resistance matrix $G_{k \rightarrow N}$ of the remaining piece of the flagellum, namely the ensemble of the last $N - k + 1$ rods. Actually, we need just the third column of $G_{k \rightarrow N}$, since the element $(0, 0, 1)$ of the Lie algebra $sE(2)$ represents unit rotation around a hinge. Multiplying on the left by $M(x_k, y_k, \phi_k)^\dagger$, we refer this torque and force to the cell’s center (the reference point).

Finally, in order to evaluate $k_{ij} = \langle X_i, X_j \rangle$ we explore the orthogonality between horizontal and vertical subspaces. We have

$$\langle X_i, X_j \rangle = \left\langle \frac{\partial}{\partial \theta_i}, \frac{\partial}{\partial \theta_j} \right\rangle + \left\langle c_{1j} \frac{\partial}{\partial x} + c_{2j} \frac{\partial}{\partial y} + c_{3j} \frac{\partial}{\partial \phi}, \frac{\partial}{\partial \theta_i} \right\rangle,$$

or equivalently,

$$\langle X_i, X_j \rangle = \left\langle \frac{\partial}{\partial \theta_i}, \frac{\partial}{\partial \theta_j} \right\rangle + \left\langle c_{1i} \frac{\partial}{\partial x} + c_{2i} \frac{\partial}{\partial y} + c_{3i} \frac{\partial}{\partial \phi}, \frac{\partial}{\partial \theta_j} \right\rangle.$$

The inner products appearing above,

$$\left\langle \frac{\partial}{\partial \theta_i}, \frac{\partial}{\partial \theta_j} \right\rangle, \left\langle \frac{\partial}{\partial \theta_j}, \frac{\partial}{\partial x} \right\rangle, \left\langle \frac{\partial}{\partial \theta_j}, \frac{\partial}{\partial y} \right\rangle, \left\langle \frac{\partial}{\partial \theta_j}, \frac{\partial}{\partial \phi} \right\rangle$$

can be obtained by the matrix algebra rules in section 2. We must compute the contribution of each of the $N + 1$ rods $k = 0, \dots, N$. At rod k , we refer the velocity vectors to its left-end point, and we use matrix G_o given by (15) to calculate the inner products.

More precisely, let us show how $\langle \partial/\partial \theta_j, V \rangle$ are calculated. Here V is any one of the vectorfields $\partial/\partial \theta_i, \partial/\partial x, \partial/\partial y, \partial/\partial \phi$.

First of all, only the rods a_k with $k \geq j$ contribute, because the action of $\partial/\partial \theta_j$ does not affect the previous rods. In fact, this action consists on the rotation with unit angular velocity around hinge j of the “frozen” subsequent links. This element of $sE(2)$ is represented in the frame of rod k by

$$R(-\phi_k)T(O_k - O_j)(0, 0, 1)^\dagger$$

The vectorfields $\partial/\partial x$ and $\partial/\partial y$ do not change their form, i.e., are represented for all rods by $(1, 0, 0)$ and $(0, 1, 0)$. The vectorfield $\partial/\partial \phi$ is represented in the frame of rod k as

$$R(-\phi_k)T(O_k)(0, 0, 1)^\dagger$$

Thus, for instance

$$\langle \partial/\partial \theta_j, \partial/\partial \phi \rangle = \sum_{k \geq j} (0, 0, 1)T^\dagger(O_k)R(\phi_k)G_oR(-\phi_k)T(O_k - O_j)(0, 0, 1)^\dagger$$

or equivalently

$$\langle \partial/\partial \theta_j, \partial/\partial \phi \rangle = \sum_{k \geq j} [T^\dagger(O_k)R(\phi_k)G_oR(-\phi_k)T(O_k - O_j)]_{33}.$$

The calculation of $\langle \partial/\partial \theta_i, \partial/\partial \theta_j \rangle$ goes along similar lines. Note that only rods a_k with $k \geq \max\{i, j\}$ contribute, and we just showed how rotations around one hinge are represented when seen in the frame of another one.

We can provide a Matlab .m file for the interested reader.

6. SIMULATIONS

We present the results of three numerical simulations. The first is just a check, taking $a_2 = 0$, and the result (See Table 1) verifies Purcell's oyster paradox. Simulations 2 and 3 describe the locomotion of Purcell's animat (with three equal segments of length 1) through a cycle in shape space where the maximum absolute value of the angles between the segments is $\alpha = \pi/4$ and $\alpha = \pi/40$, respectively. Note the factor of $1/100$.

The parameters are $a_k = 1, r = 0, C_N = 2, C_T = 1$. The motion plan is given by

$$\theta_1 = \alpha \cos(t) \quad , \quad \theta_2 = \alpha \sin(t) \quad .$$

Data from the second and third columns of Tables 2 and 3 are depicted in Fig. 5 and Fig. 6. We draw only the (x, y) positions of the left hand point O .

Note that the net y displacement is zero (up to numerical error, we have not worried about streamlining the ODE solver), but the motion is somewhat skewed. This feature disappears if one depicts the motion of the middle point of the second segment. Note also that the animat seems to move like a basketball or soccer player, dribbling back and forward during the cycle. The net x motion is in the *negative* direction (although it starts moving in the positive x -direction). This confirms Purcell's intuition. We got the opposite direction of what he says, but remember that our cycle is traversed in *reciprocal time*, so everything fits.

Quantitatively, note that the net x displacement for the second simulation is almost exactly $1/100$ of the first. Again, this fits well with the geometrical insight, since the area in the shape space was reduced by this factor. The net locomotion in Table 2 is about $1/30$ of the total length, so if the flagellum does 60 cycles per second (this is the order of magnitude on a flagellum) it will move 2 lengths per second, which is roughly what is observed in spermatozoa.

TABLE 1.
Scallop: $\alpha_2 = 0$ ($\alpha = \pi/4$).

t	x	y	ϕ
* 0	0	0	-1.5707963
0.00005	0.00002	-0.00001	-1.5708357
0.00045	0.00023	-0.00011	-1.5711513
0.00246	0.00128	-0.00064	-1.5727273
0.01250	0.00651	-0.00329	-1.5805593
0.06274	0.03191	-0.01690	-1.6184996
0.31393	0.13779	-0.08569	-1.7749479
0.94199	0.21126	-0.14365	-1.8825258
** 1.57031	0.00025	0.00000	-1.57116964
2.19863	-0.36085	0.03195	-0.9596754
2.82694	-0.50802	-0.26965	-0.2816133
3.455268	-0.36506	-0.58839	0.2040200
4.08358	-0.30704	-0.66196	0.3117292
4.71190	-0.45069	-0.45095	0.0003730
5.34022	-0.48265	-0.08984	-0.6111211
5.49730	-0.43264	-0.01840	-0.7848622
5.65438	-0.36133	0.03174	-0.9586152
5.81146	-0.27484	0.05712	-1.1281185
5.92939	-0.20469	0.05954	-1.2500479
6.047323	-0.13366	0.04917	-1.3655193
6.165254	-0.06463	0.02831	-1.4729317
** 6.28318	-0.00000	-0.00000	-1.5707963

NOTES

* This simulation is only a check.

** After the full cycle, there is no net motions.

TABLE 2.
Purcell's animat, no cell: $a_1 = a_2 = a_3 = 1$ $\alpha = \pi/4$.

* t	x	y	ϕ
0	0	0	-0.78539
0.00010	0.00001	0.00001	-0.78542
0.00070	0.00007	0.00010	-0.78555
0.00371	0.00041	0.00054	-0.78620
0.01878	0.00205	0.00271	-0.78940
0.09414	0.00947	0.01267	-0.80329
0.47092	0.02257	0.03977	-0.81812
1.09907	-0.04643	-0.00435	-0.65031
1.72739	-0.15950	-0.16238	-0.32124
2.51279	-0.21050	-0.44240	0.13315
3.14110	-0.18101	-0.61164	0.37342
3.61234	-0.17621	-0.65721	0.40628
4.08358	-0.20699	-0.61968	0.30002
4.5548	-0.24894	-0.50521	0.08667
5.02606	-0.26051	-0.34158	-0.1841
5.49730	-0.21982	-0.17219	-0.46083
5.92939	-0.15215	-0.04713	-0.67282
6.16525	-0.11656	0.00212	-0.75546
** 6.28318	-0.10195	0.02129	-0.78539

NOTES

* This simulation runs in the opposite time direction from Purcell's.

** After the full cycle, there is a net x motion of about 1/30 of the length.

TABLE 3.
Purcell's animat, no cell: $\mathbf{a}_1 = \mathbf{a}_2 = \mathbf{a}_3 = 1$ $\alpha = \pi/40$.

* t	x	y	ϕ
0	0	0	-0.078539816
0.000050237	0.000000057	0.000000875	-0.078540839
0.000100475	0.000000114	0.000001750	-0.078541863
0.000452139	0.000000516	0.000007875	-0.078549023
0.001205705	0.000001375	0.000020985	-0.078564342
0.004973535	0.000005650	0.000086239	-0.078640442
0.018788910	0.000021032	0.000321257	-0.078912384
0.062746923	0.000066796	0.001024211	-0.079703039
0.156942664	0.00014732	0.002295835	-0.081009390
0.627921370	0.000129396	0.003598647	-0.079407504
1.570312435	-0.001489793	-0.017373982	-0.040756029
2.041551333	-0.002163585	-0.035101757	-0.012134206
2.512790231	-0.002307672	-0.052781546	0.014697665
3.455268027	-0.001945127	-0.073408339	0.041258741
4.397745823	-0.002573515	-0.062230378	0.017002137
4.868984721	-0.002843567	-0.046631056	-0.009319842
5.340223619	-0.002608495	-0.028465369	-0.038047271
5.811462517	-0.001912090	-0.011700216	-0.062925285
5.929393215	-0.001712180	-0.008170896	-0.067876081
6.165254609	-0.001344475	-0.002267958	-0.075738010
6.283185307	-0.001194395	0.000024324	-0.078539813

NOTES

* This simulation runs in the opposite time direction from Purcell's.

** After the full cycle, there is a net x motion of about 1/100 of the previous.

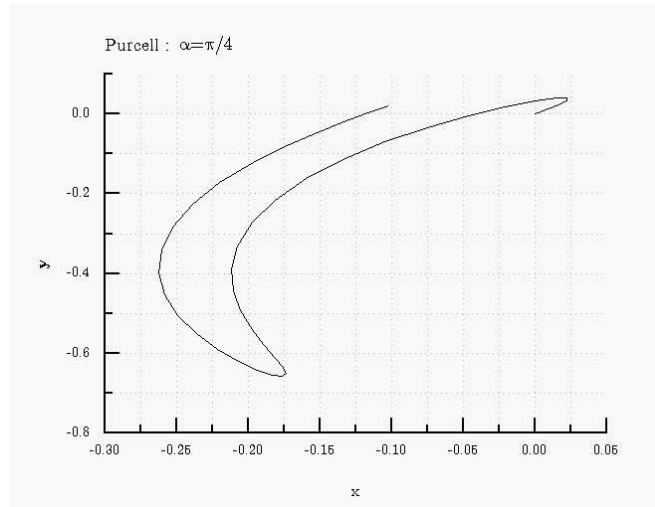


FIG. 5. (x, y) values for one cycle (no cell). Here $\alpha = \pi/4$.

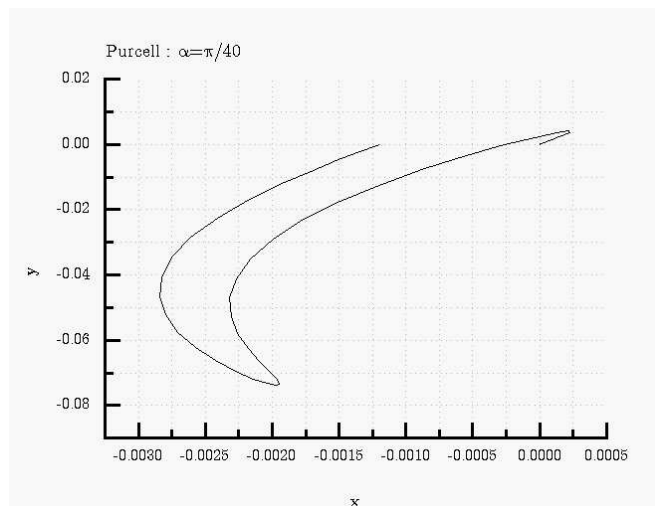


FIG. 6. (x, y) values one cycle (no cell). Here $\alpha = \pi/40$.

7. CONCLUSIONS AND DIRECTIONS.

We presented in this paper: i) a simple method not only to describe the kinematics of flagellary locomotion; ii) the Hamiltonian for the optimal motions, using sub-Riemannian geometry. For simplicity, we modeled the flagellum as a sequence of concatenated segments. The description can be easily extended for the case of a continuous flagellum; presently (work in progress) we are studying flagellary motions where, at any given time snapshot, the flagellum has the shape of concatenated circular arcs [15, 9].

Observe that all that matters for the fundamental connection formula of self propulsion (27) is the ratio C_N/C_T between the resistance coefficients, and not their actual values. *For this reason, we believe that the the results using the resistive theory will be essentially the same as using more refined fluid dynamical treatment.*

At any rate, efficient numerical methods for Stokes flows are available, based either on boundary integral formulations [38] or distributions of singularities (along the flagellum centerline). A comparison is in order. In particular, Lighthill's method of singularities [29] is accurate to second order in the *slenderness*, the ratio of the flagellum diameter to total length, and has been recently extended by Liron [30] to multi-cilia configurations.

Recent discoveries (since about ten years ago) in cell biology spurred a surge of interest on the physical modeling of *molecular motors* [46, 34]. The molecular motor *dynein* is responsible for the microtubule sliding inside the flagellar axoneme [49]. *A more refined use of fluid mechanics, as suggested by Lighthill, may allow to deduce the location and intensities of the dynein action from knowing merely the kinematical data?*

We finish by quoting the prophetic statement by J. Lighthill in [27], p. 165:

“It is therefore arguable that the results of any calculations in flagellar hydrodynamics should, where possible, be given in two forms: on the one hand in terms of a “best possible representation through resistance coefficients”, and on the other hand in any fuller and more accurate manner such as may be achieved through any more complicated method of representation, possibly for use in studies of a more refined nature.”

Steps in this direction have been achieved by Lisa Fauci and collaborators, using Peskin's immersed boundary approach for Navier-Stokes equations [14]. In the context of Stokes equations (zero Reynolds), we think that it is possible to justify Peskin's method from first principles (presently, in the immersed boundary method, a Navier-Stokes numerical solver is used). Our idea is to model the hydrodynamical dissipation as a Rayleigh function, in addition to the conservative Lagrangian modeling the axoneme.

APPENDIX: A MATLAB FILE FOR PURCELL'S ANIMAT.

```

% command to be used in Matlab prompt:
% [T,Y] = ode45(@xyphidot,[0, 2*pi],[0 0 0 -alpha],
%             [],a1,a2,a3,ct,cn,alpha,r)
% alternative: use quad to integrate phidot, xdot, ydot
% -----
function dy = xyphidot(t,y,a1,a2,a3,ct,cn,alpha,r)
% parameter alpha in [0,pi] "size" of shape space disk
dy = zeros(4,1);
R = zeros(3,3);
%       shape space curve
%       one can make many other choices)
%       theta1 = alpha * cos(y(1));
%       theta2 = alpha * sin(y(1)) ;
%       theta1dot = - alpha * sin(y(1));
%       theta2dot = alpha * cos(y(1)) ;
% matrix H 3X2 of UNlocalized Hinges
% H = [x1 y1; x2 y2; x3 y3];
phi1 = theta1;
phi2 = theta1 + theta2;
x1 = a1;
y1 = 0;
x2 = x1 + a2 * cos(phi1) ;
y2 = y1 + a2 * sin(phi1) ;
% x3 = x2 + a3 * cos(phi2);
% y3 = y2 + a3 * sin(phi2);
% Resistance matrices
Go = [6*pi*r 0 0; 0 6*pi*r 0; 0 0 8*pi*(r^3)];
% cell resistance matrix
G1 = [a1*ct 0 0; 0 a1*cn (a1^2)*cn/2;
      0 (a1^2)*cn/2 (a1^3)*cn/3];
G2 = [a2*ct 0 0; 0 a2*cn (a2^2)*cn/2;
      0 (a2^2)*cn/2 (a2^3)*cn/3];
G3 = [a3*ct 0 0; 0 a3*cn (a3^2)*cn/2;
      0 (a3^2)*cn/2 (a3^3)*cn/3];
T1 = [1 0 -y1; 0 1 x1; 0 0 1];
T2 = [1 0 -y2; 0 1 x2; 0 0 1];
T12 = [1 0 0; 0 1 a2; 0 0 1];
R1 = [cos(phi1) -sin(phi1) 0; sin(phi1) cos(phi1) 0; 0 0 1];
R2 = [cos(phi2) -sin(phi2) 0; sin(phi2) cos(phi2) 0; 0 0 1];
R12 = [cos(theta2) -sin(theta2) 0;
       sin(theta2) cos(theta2) 0; 0 0 1];

```

```

% -----
% resistance matrix and its inverse
G = G0 + G1 + T1'*R1*G2*R1'*T1 + T2'*R2*G3*R2'*T2;
GINV = [1 0 0; 0 1 0; 0 0 1]/G
% force matrix A and connection matrix C
GG = G2 + T12'*R12*G3*R12'*T12;
A1 = T1'*R1*GG*[0;0;1];
A2 = T2'*R2*G3*[0;0;1];
C1 = - GINV*A1;
C2 = - GINV*A2;
C = [C1(1),C2(1); C1(2) C2(2); C1(3) C2(3)];
% -----
% control rule at standard gauge
R = [cos(y(4)) -sin(y(4)) 0 ; sin(y(4)) cos(y(4)) 0 ; 0 0 1];
CC = C * [theta1dot ; theta2dot];
dy = [1; R*CC];

```

ACKNOWLEDGMENT

(GA) thanks the Women's Program in Mathematics, Institute of Advanced Study, for sponsoring her participation in the 2003 Biomathematics Workshop. (JK) thanks Richard Murray and Jerry Marsden for sponsoring a visit to Control and Dynamical Systems/Caltech, Fall and Winter 2001-2002. Thanks to the CDS students and staff for the wonderful atmosphere, and to Joel Burdick's group for their inspiring "zoobotics" seminar. Thanks to Waldyr Oliva and Carlos Rocha for their hospitality at the Instituto Superior Tecnico, Lisbon, June 2003.

REFERENCES

1. V.I. ARNOLD, V.V. KOZLOV, AND A.I. NEISHTADT, *Dynamical Systems III*, (*Encyclopaedia of Mathematical Sciences*, vol. **3**, Springer, New York 1988).
2. L.E. BECKER, S.A. KOEHLER AND H.A. STONE, *On self-propulsion of micro-machines at low Reynolds number: Purcell's three-link swimmer*, submitted to J. Fluid. Mech.
3. J. R. BLAKE, *A spherical envelope approach to ciliary propulsion*, J.Fluid Mech. **46**, 199–208 (1971).
4. J.R. BLAKE, *Self propulsion due to oscillations on the surface of a cylinder at low Reynolds number*, Bull.Austral.Math.Soc.**3**, 255–264 (1971).
5. J.R. BLAKE, *Infinite models for ciliary propulsion*, J.Fluid Mech. **49**, 209–222 (1971).
6. J.R. BLAKE, *A model for the micro-structure in ciliated organisms*, J.Fluid Mech. **55**, 1–23 (1972).
7. C. BRENNEN, *An oscillating boundary layer theory for ciliary propulsion*, J.Fluid Mech. **65**, 799–824 (1974).
8. C. BRENNEN, H. WINNET, *Fluid Mechanics of propulsion by cilia and flagella*, Ann.Rev.Fluid Mech. **9**, 339–398 (1977).

9. C. BROKAW, *Descriptive and mechanistic models of flagellar motility*, p. 128–139, in W. Alt, G. Hoffmann, eds., *Biological Motion* (Springer Verlag Lecture Notes in Biomathematics, **89**, 1990).
10. C. BROKAW, *Control of flagellar bending: a new agenda based on dynein diversity*, Cell Motil. Cytosk. **28**, 199–204 (1994).
11. R.G. BROWN, <http://www.phy.duke.edu/rgb/Class/phy41/node11.html>
12. K. EHLERS, *The Geometry of Swimming and Pumping at Low Reynolds number* (Ph.D. Thesis, Univ. of Calif., Santa Cruz, 1995).
13. K. EHLERS, A. SAMUEL, H. BERG, R. MONTGOMERY, *Do cyanobacteria swim using traveling surface waves?*, Proc. Nat. Acad. Sci, **93** 8340–8343 (1996).
14. L.J. FAUCI, S. GUERON (EDITORS), *Computational Modeling in Biological Fluid Dynamics* (Springer Verlag IMA Volumes in Mathematics and Its Applications, **124**, 2001).
15. S.F.GOLDSTEIN, *Morphology of developing bends in sperm flagella*, p. 127–132., in T.Y. Wu, C. Brennen, C. Brokaw, eds. *Swimming and Flying in Nature*, (Plenum Press, New York, 1975), vol.1 .
16. J. HAPPEL, H. BRENNER, *Low Reynolds number Hydrodynamics* (Kluwer Acad. Pub., 1991).
17. H. HERTZ, *The principles of mechanics, presented in a new form. Pref. by H. von Helmholtz*, (Dover Publications, New York, 1956).
18. J.J.L. HIGDON, *The generation of feeding currents by flagellar motions*, J.Fluid Mech. **94**:2, 305–330 (1979).
19. S.T. KELLER, T.Y. WU, *A porous prolate-spheroidal model for ciliated microorganisms*, J.Fluid Mech. **80**:2, 259–278 (1977).
20. J. KOILLER, R. MONTGOMERY AND K. EHLERS, *Problems and progress in Microswimming*, J.Nonlinear Science **6**, 507–541 (1996).
21. J. KOILLER, M. A. RAUPP, J.DELGADO, K. EHLERS AND R. MONTGOMERY, *Spectral methods for Stokes flows*, Computational and Applied Mathematics, **17**:3, 343–371 (1998).
22. J. KOILLER, J. DELGADO, *On efficiency calculations for nonholonomic locomotion problems: an application to microswimming*, Rep. Math. Phys.**42**, no. 1-2, 165–183 (1998).
23. J. KOILLER, K. EHLERS, A. CHERMAN, J. DELGADO, R. MONTGOMERY AND F. DUDA, *Low Reynolds Number Swimming in Two Dimensions, Proceedings of the III International Symposium of Hamiltonian Systems and Celestial Mechanics (MAMSYS98)*, (World Scientific Monograph Series in Mathematics - Vol. 6, ed. by J. Delgado, E. A. Lacomba, E. Prez-Chavela, World Scientific, Singapore, 2000).
24. J.KOILLER, ET AL., THE E. COLI COLLECTIVE, *Momentum Maps and Geometric Phases*, in H. Cabral and F. Diacu eds., *Classical and Celestial Mechanics* (Princeton U. Press, New Jersey, 2002).
25. J. LIGHTHILL, *On the squirming motion of nearly spherical deformable bodies through liquids at very small Reynolds number*, Commun. Pure Appl. Math. **5**, 109–118 (1952).
26. J. LIGHTHILL, *Mathematical Biofluidmechanics* (SIAM, Philadelphia, PA, 1975).
27. J. LIGHTHILL, *Flagellar hydrodynamics*, SIAM Review **18**, 161–230 (1976).
28. J. LIGHTHILL, *Biofluidynamics: a survey*, in Contemp. Math, **141**, 1–23, ed. by A.Y.Cheer, C.P.van Dam (1993).

29. J. LIGHTHILL, *Reinterpreting the basic theorem of flagellar hydrodynamics*, J. Eng. Math. **30**, 25–34 (1996).
30. N. LIRON, *The LDL theorem - historical perspective and critique*, p. 1533-1540, in *Biofluidynamics: in memory of Sir James Lighthill* (J. Wiley Math. Methods Appl. Sci. **24**, 17–18, 2001).
31. J.E. MARSDEN, T. RATIU, *Introduction to Mechanics and Symmetry: A Basic Exposition of Classical Mechanical Systems* (Springer Texts in Applied Mathematics **17**, 1999).
32. R. MONTGOMERY, *A Tour of Subriemannian Geometries, Their Geodesics and Applications*, (American Mathematical Society Mathematical Surveys and Monographs **91**, 2002).
33. R. MONTGOMERY, *Nonholonomic control and gauge theory*, in *Nonholonomic Motion Planning*, ed. by Li,Z., Canny, J.F., Kluwer (1993).
34. G. OSTER, *Darwin's Motors*, Nature **417**, 25 (2002).
35. O. PIRONNEAU, D.F. KATZ, *Optimal swimming motions of flagella*, in *Swimming and Flying in Nature*, (Plenum Press, New York, 1975), vol.1,ed. by T.Y. Wu, C. Brennen, C. Brokaw, p. 161–170.
36. O. PIRONNEAU, D.F. KATZ, *Optimal swimming of flagellated micro-organisms*, J. Fluid Mechanics **66**, part 2, 391–425 (1974).
37. M. PORTER, W. SALE, *The 9+2 axoneme anchors multiple inner arm dyneins and a network of kinases and phosphatases that control motility*, J. Cell. Biol. **151**:5, F37–F42 (2000).
38. C. POZRIKIDS, *Boundary Integral and Singularity Methods for Linearized Viscous flow* (Cambridge Texts in Applied Mathematics, 1992).
39. E. PURCELL, *Life at low Reynolds number*, Amer.J. Phys. **45**, 3–11 (1977).
40. E. PURCELL, *The efficiency of propulsion by a rotating flagellum*, Proc. Natl. Acad. Sci. USA **94**, 11307–11311 (1997).
41. P. SATIR, *The cilium as a biological nanomachine*, FASEB J. **13**, S235–S237 (1999).
42. P. SATIR, *Control molecules in Protozoan Ciliary Motility*, Jpn. J. Protozool **36**:2, 87–96 (2003).
43. A. SHAPER, *Gauge Theory of Deformable Bodies: A Theory of Something*, (Ph.D. thesis, Princeton University Physics Department, 1989).
44. A. SHAPER AND F. WILCZEK, F., *Geometry of self-propulsion at low Reynolds number*, J.Fluid Mech. **198**, 557–585 (1989).
45. A. SHAPER AND F. WILCZEK, *Efficiencies of self-propulsion at low Reynolds number*, J.Fluid Mech. **198**, 587–599 (1989).
46. M. SCHLIWA, *Molecular Motors* (J. Wiley, 2003).
47. P. SUGRUE, J. AVOLIO, P. SATIR AND M.E. HOLWILL, *Computer modelling of Tetrahymena axonemes at macromolecular resolution. Interpretation of electron micrographs*, Journal of Cell Science, Vol 98, Issue 1, 5–16 (1991).
48. G.I. TAYLOR, *Analysis of the swimming of microscopic organisms*, Proc.R.Soc.Lond.A **209**, 447–461 (1951).
49. H.C.TAYLOR, P.SATIR, M.HOLWILL, *Assessment of inner dynein arm structure and possible function in ciliary and flagellar axonemes*, Cell Motil. Cytoskel. **43**, 167–177 (1999). See also <http://www.wadsworth.org/albcon97/abstract/holwill.htm>, <http://www.wadsworth.org/albcon97/abstract/guevara.htm> .
50. T.Y. WU, C. BRENNEN, C. BROKAW, eds. *Swimming and Flying in Nature*, (Plenum Press, New York, 1975), vol.1 .